

Impacts of Pavement Adhesion Coefficient on Parallel Regenerative Braking Strategy of PHEV

Jingming Zhang¹, Jinlong Liu^{1*}, Jiawei Ma², Xiaoyu Zhang³, Zhiwei Gao⁴

¹School of Automotive Engineering, Harbin Institute of Technology, Weihai, 264209, China;

²School of Engineering, Melbourne University, Melbourne, 3010, Australia;

³School of Astronautics, Harbin Institute of Technology, Harbin, 150001, China;

⁴Department of Environment Protection in Zhenglu Town, Changzhou, 213111, China

Abstract. The parallel hybrid electric vehicles (PHEV) are becoming one of the hottest topics in automobile industry. In order to have more deeply understanding in parallel regenerative braking strategy, the impacts of pavement adhesion coefficient on it were discussed. The impacts on regenerative braking recovery rate and braking distance were studied through theoretical derivations. The braking models were established and simulated on the platform of MATLAB/SIMULINK. The results indicate that the recovery rate increases with increment of pavement adhesion coefficient when the pavement adhesion coefficient is lower than 0.7 and that the recovery rate remains unchanged when the pavement adhesion coefficient is higher than 0.7. Additionally, the braking distance decreases with the increment of pavement adhesion coefficient.

Keywords: Parallel hybrid electric vehicles, Pavement adhesion coefficient, Parallel regenerative braking strategy, Recovery rate, braking distance.

1. Introduction

Hybrid electric vehicles, transitional products between internal-combustion engine vehicles (ICEVs) and pure electric vehicles, would become the main products in automobile plants [1-2]. This is because they not only alleviate the serious crisis of oil shortage and environmental pollution caused by ICEVs but also address the storage problems of cells in electric cars [3-4]. Influencing factors of regenerative braking should be studied, thereby understanding its performances deeply [5-6]. Pavement adhesion coefficient is the static friction coefficient between tires and pavement. Its value is determined by the road type, drying degree, tire structure and tread pattern. The pavement adhesion coefficient has great influences on the regenerative braking.

2. Parallel regenerative braking strategy

The parallel strategy divides the braking process into three parts. When the expected braking severity is lower than 0.1, the PHEV is in mild braking period. When the expected braking severity is higher than 0.1 but lower than 0.7 and the mechanical braking forces have not made the front or rear wheels being in critical locked state, the PHEV is in moderate braking period. When the braking severity is higher than 0.7 or the mechanical braking forces have made the front or rear wheels being in critical locked state, the PHEV is in severe braking period.

In the parallel strategy, the ratio of front mechanical braking force to rear mechanical braking force is a constant value.

$$\beta_{me} = \frac{F_{b_f_me}}{F_{b_f_me} + F_{b_r_me}} \quad (1)$$

As is shown in the Eq.1, β_{me} is the mechanical braking force distribution coefficient; $F_{b_f_me}$ is the mechanical braking force on front wheels; $F_{b_r_me}$ is the mechanical braking force on rear wheels.

The mechanical braking force distribution is determined by the vehicle parameters and the synchronizing adhesion coefficient.

$$\varphi_0 = (L\beta_{me} - b) / h_g = [(a+b)\beta_{me} - b] / h_g \quad (2)$$

As is shown in the Eq.2, φ_0 is the synchronizing adhesion coefficient; a is the distance between center of mass and front axle; b is the distance between center of mass and rear axle; h_g is the height of center of mass; L is the wheel base of vehicle.

The mechanical braking force is determined by the driver intention; while the regenerative braking force is determined by the drive type.

In the mild braking period, only the regenerative braking forces play roles in braking process. In the moderate braking period, both the regenerative braking forces and the mechanical braking forces play roles in braking process. In the severe braking period, only the mechanical braking forces play roles in braking process.

2.1 Passenger vehicle with front-wheel drive pattern

The regenerative braking forces are added on front wheels in passenger vehicle with front-wheel drive pattern.

$$F_{b_f_sum} = F_{b_f_me} + F_{b_f_re} \quad (3)$$

$$F_{b_r_sum} = F_{b_r_me} \quad (4)$$

As is shown in Eq.3 and Eq.4: $F_{b_f_sum}$ is the sum of braking force on front wheels; $F_{b_r_sum}$ is the sum of braking force on rear wheels; $F_{b_f_re}$ is the participant regenerative braking force on front wheels.

The braking force distribution coefficient of PHEV with front-wheel drive pattern is the ratio of the sum of front mechanical braking force and front regenerative braking force to the sum of mechanical braking force and regenerative braking force.

$$\beta_{hev_f} = \frac{F_{b_f_me} + F_{b_f_re}}{F_{b_f_me} + F_{b_r_me} + F_{b_f_re}} \quad (5)$$

As is shown in Eq.5, β_{hev_f} is the braking force distribution coefficient of PHEV with front-wheel pattern.

In the mild braking period, the regenerative braking forces are added on front wheels and the mechanical braking forces of front and rear wheels are zero.

$$F_{b_f_re} = F_{re_a} \quad (6)$$

$$F_{b_f_me} = F_{b_r_me} = 0 \quad (7)$$

As is shown in Eq.6, F_{re_a} are the maximum regenerative braking forces that are provided by the motor.

In the moderate braking period, both the regenerative braking forces and the mechanical braking forces contribute to the braking operation. The value of regenerative braking force is decided by the ECE braking regulations and the constraint of anti-lock front wheels.

The limitations of ECE braking regulations reflect in the braking force distribution coefficient.

$$\beta_{hev_f_max} = (b + zh_g)(z + 0.07) / (0.85Lz) \quad (8)$$

As is shown in Eq.8, $\beta_{hev_f_max}$ is the maximum braking force distribution coefficient allowed by ECE; z is the severity of braking.

$$F_{b_f_re} \leq \frac{(\beta_{hev_f_max} - 1)F_{b_f_me} + \beta_{hev_f_max}F_{b_r_me}}{1 - \beta_{hev_f_max}} = F_{b_f_re_ECE} \quad (9)$$

As is shown in Eq.9, $F_{b_f_re_max}$ is the maximum regenerative braking force on front wheels allowed by ECE.

The constraints of anti-lock front wheels can be concluded by the f curve.

$$F_{b_f_lock} = \frac{F_{b_r_sum} + Gb / h_g}{(L - \varphi h_g) / \varphi h_g} \tag{10}$$

$$F_{b_f_re} \leq F_{b_f_lock} - F_{b_f_me} = F_{b_f_re_ABS} \tag{11}$$

As is shown in Eq.10 and Eq.11, $F_{b_f_lock}$ is the maximum braking force on front wheels allowed by anti-lock front wheels constraint; φ is the pavement friction coefficient; G is the vehicle gravity; $F_{b_f_re_ABS}$ is the maximum regenerative braking force on front wheel allowed by anti-lock front wheels constraint.

Eq. 12 shows the maximum regenerative braking force in the moderate braking period.

$$F_{b_f_re_max} = \min \{ F_{b_f_re_ECE}, F_{b_f_re_ABS} \} \tag{12}$$

Eq.13 shows the participant regenerative braking force in the moderate braking period.

$$F_{b_f_re} = \begin{cases} F_{re_a}, & F_{re_a} \leq F_{b_f_re_max} \\ F_{b_f_re_max}, & F_{re_a} > F_{b_f_re_max} \end{cases} \tag{13}$$

In the severe braking period, only the mechanical braking forces play roles in braking process; the regenerative braking force is zero.

$$F_{b_f_re} = 0 \tag{14}$$

2.2 Commercial vehicle with rear-wheel drive pattern

The regenerative braking forces are added on rear wheels in commercial vehicle with rear-wheel drive pattern.

$$F_{b_f_sum} = F_{b_f_me} \tag{15}$$

$$F_{b_r_sum} = F_{b_r_me} + F_{b_r_re} \tag{16}$$

As is shown in Eq.16: $F_{b_r_re}$ is the participant regenerative braking force on rear wheels.

The braking force distribution coefficient of PHEV with rear-wheel drive pattern is the ratio of the front mechanical braking force to the sum of mechanical braking force and regenerative braking force.

$$\beta_{hev_r} = \frac{F_{b_f_me}}{F_{b_f_me} + F_{b_r_me} + F_{b_r_re}} \tag{17}$$

As is shown in Eq.17, β_{hev_r} is the braking force distribution coefficient of PHEV with rear-wheel pattern.

In the mild braking period, the regenerative braking forces are added on rear wheels and the mechanical braking forces of front and rear wheels are zero.

$$F_{b_r_re} = F_{re_a} \tag{18}$$

$$F_{b_f_me} = F_{b_r_me} = 0 \tag{19}$$

In the moderate braking period, both the regenerative braking forces and the mechanical braking forces contribute to the braking operation. The value of regenerative braking force is decided by the ECE braking regulations and the constraint of anti-lock front wheels.

The limitations of ECE braking regulations reflect in the braking force distribution coefficient. Table 1 shows the limitations.

Table 1 Lower limit value of braking force distribution coefficient

Braking severity	Lower limit value of braking force distribution coefficient
$0.1 \leq z < 0.15$	$(b + zh_g) / L$
$0.15 \leq z \leq 0.3$	$\max \left\{ (z - 0.08)(b + zh_g) / Lz, \left[1 - (z - 0.08)(a - zh_g) / Lz \right], (b + zh_g) / L \right\}$
$0.3 < z \leq 0.6$	$\max \left\{ \left[1 - (z - 0.0188)(a - zh_g) / (0.74Lz) \right], (b + zh_g) / L \right\}$
$z > 0.6$	$\left[1 - (z - 0.0188)(a - zh_g) / (0.74Lz) \right]$

Eq.20 shows the maximum regenerative braking force on rear wheels allowed by ECE.

$$F_{b_r_re} \leq \frac{(1 - \beta_{hev_r_min}) F_{b_f_me} - \beta_{hev_r_min} F_{b_r_me}}{\beta_{hev_r_min}} = F_{b_r_re_ECE} \quad (20)$$

As is shown in Eq.20, $\beta_{hev_r_min}$ is the minimum braking force distribution coefficient allowed by ECE; $F_{b_r_re_max}$ is the maximum regenerative braking force on rear wheels allowed by ECE.

The constraints of anti-lock rear wheels can be concluded by the r curve.

$$F_{b_r_lock} = \frac{\varphi G a}{L + \varphi h_g} - \frac{\varphi h_g}{L + \varphi h_g} F_{b_f_sum} \quad (21)$$

$$F_{b_r_re} \leq F_{b_r_lock} - F_{b_r_me} = F_{b_r_re_ABS} \quad (22)$$

As is shown in Eq.21 and Eq.22, $F_{b_r_lock}$ is the maximum braking force on rear wheels allowed by anti-lock rear wheels constraint; $F_{b_r_re_ABS}$ is the maximum regenerative braking force on rear wheel allowed by anti-lock rear wheels constraint.

Eq. 23 shows the maximum regenerative braking force in the moderate braking period.

$$F_{b_r_re_max} = \min \{ F_{b_r_re_ECE}, F_{b_r_re_ABS} \} \quad (23)$$

Eq.24 shows the participant regenerative braking force in the moderate braking period.

$$F_{b_r_re} = \begin{cases} F_{re_a}, & F_{re_a} \leq F_{b_r_re_max} \\ F_{b_r_re_max}, & F_{re_a} > F_{b_r_re_max} \end{cases} \quad (24)$$

In the severe braking period, only the mechanical braking forces play roles in braking process; the regenerative braking force is zero.

$$F_{b_r_re} = 0 \quad (25)$$

3. Impacts on parallel regenerative braking strategy

In the analyses of impacts, the driver intention adopts the process of slowly stepping on the brake pedal. The process of slowly stepping on the brake pedal contains the mild braking period, the moderate braking period and the severe braking period.

Fig.26 shows the relation of pavement adhesion coefficient during the analyses.

$$0.1 < \varphi_L < \varphi_H \quad (26)$$

As is shown in Fig.26: φ_L is a certain pavement adhesion coefficient; φ_H is a certain pavement adhesion coefficient and is higher than φ_L .

3.1 Impacts on recovery rate

When $0.1 < \varphi_L < \varphi_H < 0.7$, the PHEV enters the severe braking period because the mechanical braking forces make the front (rear) wheels being in the critical locked state, not because the braking severity is higher than 0.7.

In the mild braking period, the PHEV running on the road whose pavement adhesion coefficient is φ_L has the same states with the PHEV running on the road whose pavement adhesion coefficient is φ_H . So the recovered energy is equal in this period.

$$Energy_{\varphi_L_partA} = Energy_{\varphi_H_partA} \quad (27)$$

As is shown in Fig.27: $Energy_{\varphi_L_partA}$ is the recovered energy in the mild braking period when the PHEV is running on the road whose pavement adhesion coefficient is φ_L ; $Energy_{\varphi_H_partA}$ is the recovered energy in the mild braking period when the PHEV is running on the road whose pavement adhesion coefficient is φ_H .

In the moderate braking period, the PHEV running on the road whose pavement adhesion coefficient is φ_H lasts longer than the PHEV running on the road whose pavement adhesion coefficient is φ_L . In other words, the PHEV running on the road whose pavement adhesion coefficient is φ_L has the same

states with the PHEV running on the road whose pavement adhesion coefficient is φ_H before the former one finishes the moderate braking period; the PHEV running on the road whose pavement adhesion coefficient is φ_H would still stay in the moderate braking period for some time after the PHEV running on the road whose pavement adhesion coefficient is φ_L finishes the moderate braking period. Eq.28 shows the relation of the recovery rate in this period.

$$Energy_{\varphi_L - partB} < Energy_{\varphi_H - partB} \tag{28}$$

As is shown in Fig.28: $Energy_{\varphi_L - partB}$ is the recovered energy in the moderate braking period when the PHEV is running on the road whose pavement adhesion coefficient is φ_L ; $Energy_{\varphi_H - partB}$ is the recovered energy in the moderate braking period when the PHEV is running on the road whose pavement adhesion coefficient is φ_H .

In the severe braking period, they both do not recover energy.

$$Energy_{\varphi_L - partC} = Energy_{\varphi_H - partC} = 0 \tag{29}$$

As is shown in Fig.29: $Energy_{\varphi_L - partC}$ is the recovered energy in the severe braking period when the PHEV is running on the road whose pavement adhesion coefficient is φ_L ; $Energy_{\varphi_H - partC}$ is the recovered energy in the severe braking period when the PHEV is running on the road whose pavement adhesion coefficient is φ_H .

When $0.7 < \varphi_L < \varphi_H$, the PHEV enters the severe braking period because the braking severity is higher than 0.7, not because the mechanical braking forces make the front (rear) wheels being in the critical locked state.

In the mild and moderate braking periods, the PHEV running on the road whose pavement adhesion coefficient is φ_L has the same states with the PHEV running on the road whose pavement adhesion coefficient is φ_H . So the recovered energy is equal in these two periods.

$$Energy_{\varphi_L - partA} = Energy_{\varphi_H - partA} \tag{30}$$

$$Energy_{\varphi_L - partB} = Energy_{\varphi_H - partB} \tag{31}$$

In the severe braking period, they both do not recover energy.

$$Energy_{\varphi_L - partC} = Energy_{\varphi_H - partC} = 0 \tag{32}$$

Eq.33 shows the recovered energy of the PHEV running on the road whose pavement adhesion coefficient is φ_L during the whole braking process.

$$Energy_{\varphi_L} = Energy_{\varphi_L - partA} + Energy_{\varphi_L - partB} + Energy_{\varphi_L - partC} \tag{33}$$

As is shown in Eq.33, $Energy_{\varphi_L}$ is the recovered energy of the PHEV running on the road whose pavement adhesion coefficient is φ_L during the whole braking process.

Eq.34 shows the recovered energy of the PHEV running on the road whose pavement adhesion coefficient is φ_H during the whole braking process.

$$Energy_{\varphi_H} = Energy_{\varphi_H - partA} + Energy_{\varphi_H - partB} + Energy_{\varphi_H - partC} \tag{34}$$

As is shown in Eq.34, $Energy_{\varphi_H}$ is the recovered energy of the PHEV running on the road whose pavement adhesion coefficient is φ_H during the whole braking process.

Eq.35 shows the relation of the recovered energy.

$$\begin{cases} Energy_{\varphi_L} < Energy_{\varphi_H}, & 0.1 < \varphi_L < \varphi_H < 0.7 \\ Energy_{\varphi_L} = Energy_{\varphi_H}, & 0.7 \leq \varphi_L < \varphi_H \end{cases} \tag{35}$$

Eq.36 shows the relation of the recovery rate.

$$\begin{cases} \frac{Energy_{\varphi_L}}{\frac{1}{2}Mv_0^2} \leq \frac{Energy_{\varphi_H}}{\frac{1}{2}Mv_0^2}, & 0.1 < \varphi_L < \varphi_H < 0.7 \\ \frac{Energy_{\varphi_L}}{\frac{1}{2}Mv_0^2} = \frac{Energy_{\varphi_H}}{\frac{1}{2}Mv_0^2}, & 0.7 \leq \varphi_L < \varphi_H \end{cases} \quad (36)$$

As is shown in Eq.36, M is the vehicle mass; v_0 is the initial velocity.

It can be concluded from the Eq.36 that the recovery rate increases with increment of pavement adhesion coefficient until the pavement adhesion coefficient reaches the value of 0.7 and then the recovery rate remains the same.

3.2 Impacts on braking distance

The PHEV running on the road whose pavement adhesion coefficient is φ_L has the same states with the PHEV running on the road whose pavement adhesion coefficient is φ_H before the former one finishes the mild and moderate braking period. During these periods, they have the same braking severity. The braking severity of PHEV running on the road whose pavement adhesion coefficient is φ_H would be higher than the braking severity of PHEV running on the road whose pavement adhesion coefficient is φ_L after the latter one finishes the mild and moderate braking period. Eq.37 shows the relation of the braking severity.

$$\bar{z}_{\varphi_L} < \bar{z}_{\varphi_H} \quad (37)$$

As is shown in Eq.37, \bar{z}_{φ_L} is the average braking severity of the PHEV running on the road whose pavement adhesion coefficient is φ_H during the whole braking process; \bar{z}_{φ_H} is the average braking severity of the PHEV running on the road whose pavement adhesion coefficient is φ_L during the whole braking process.

Eq.38 shows the braking distance of the PHEV running on the road whose pavement adhesion coefficient is φ_L during the whole braking process.

$$Disatance_{\varphi_L} = \frac{v_0^2}{2\bar{z}_{\varphi_L}g} \quad (38)$$

As is shown in Eq.38, $Disatance_{\varphi_L}$ is the braking distance of the PHEV running on the road whose pavement adhesion coefficient is φ_L during the whole braking process.

Eq.39 shows the braking distance of the PHEV running on the road whose pavement adhesion coefficient is φ_H during the whole braking process.

$$Disatance_{\varphi_H} = \frac{v_0^2}{2\bar{z}_{\varphi_H}g} \quad (39)$$

As is shown in Eq.39, $Disatance_{\varphi_H}$ is the braking distance of the PHEV running on the road whose pavement adhesion coefficient is φ_H during the whole braking process.

Eq.40 shows the relation of the braking distance.

$$Disatance_{\varphi_L} > Disatance_{\varphi_H} \quad (40)$$

It can be concluded from the Eq.40 that the braking distance decreases with increment of pavement adhesion coefficient.

4. Braking models

The braking models of PHEV with the front-wheel drive pattern and the rear-wheel drive pattern were built on the platform of MATLAB/SIMULINK. Fig.1 shows the flow chart of the braking model of

passenger car with front-wheel drive pattern; Fig.2 shows the flow chart of the braking model of commercial car with rear-wheel drive pattern.

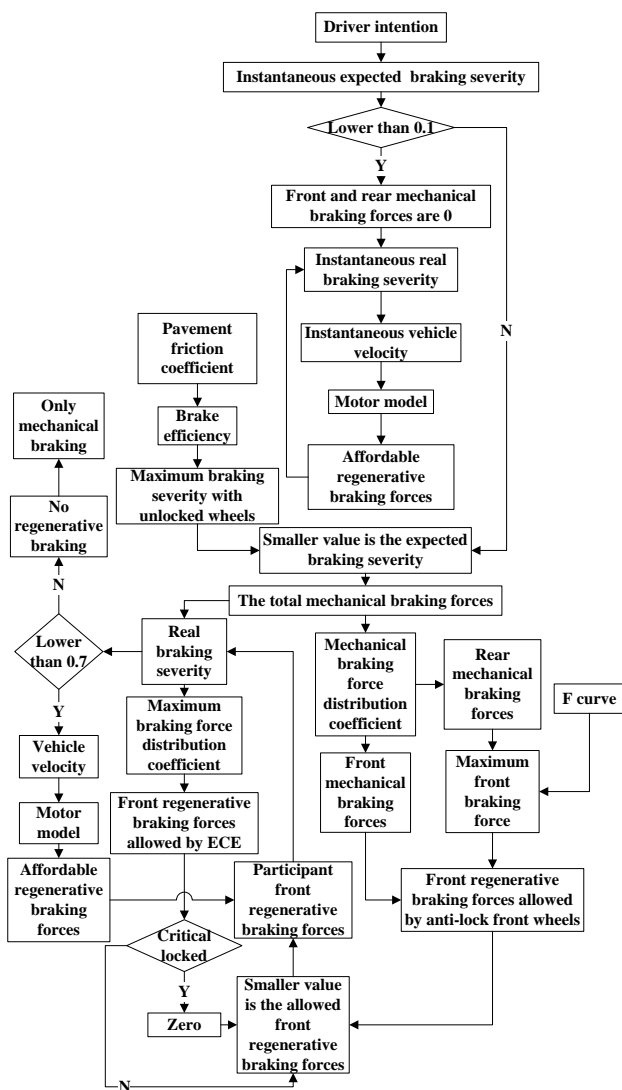


Fig.1 braking model of passenger vehicle with front-wheel drive pattern

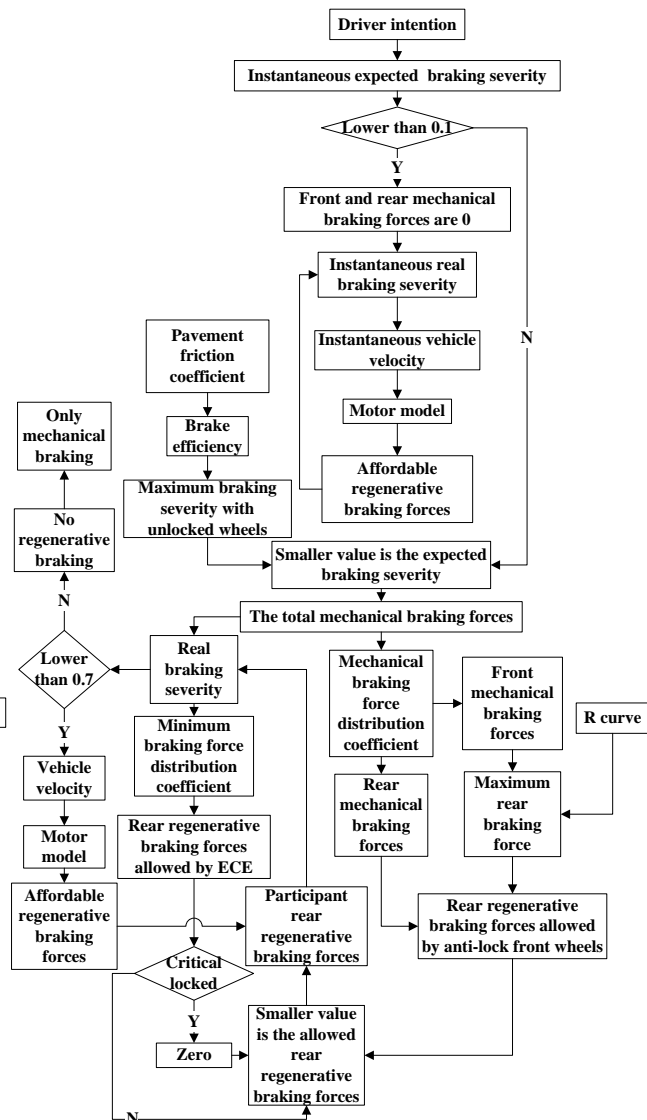


Fig.2 braking model of commercial vehicle with rear-wheel drive pattern

The model in the Fig.1 has a few differences compared with the model in the Fig.2. They were both built according to the mentioned strategies.

5. Analyses of simulation results

The model in the Fig.1, embed with the parameters shown in Table 2, was simulated. The simulation results are shown in Table 4. The model in the Fig.2, embed with the parameters shown in Table 3, was simulated. The simulation results are shown in Table 5.

Table 2 Parameters of passenger car with front-wheel drive pattern

Parameters	Value
Wheel base of PHEV [m]	2.6
Distance between front axle and the mass center [m]	1.04
Distance between rear axle and the mass center [m]	1.56
Height of center of mass [m]	0.5
Mass of PHEV [kg]	1600
Wheel radius [m]	0.25

Power of DC motor [kW]	30
Synchronizing adhesion coefficient	0.7
Mechanical braking force distribution coefficient	0.7346
Initial velocity [km/h]	50

Table 3 Parameters of commercial car with rear-wheel drive pattern

Parameters	Value
Wheel base of PHEV [m]	5.6
Distance between front axle and the mass center [m]	3.733
Distance between rear axle and the mass center [m]	1.867
Height of center of mass [m]	1
Mass of PHEV [kg]	5800
Wheel radius [m]	0.52
Power of DC motor [kW]	30
Synchronizing adhesion coefficient	0.65
Mechanical braking force distribution coefficient	0.4495
Initial velocity [km/h]	50

Table 4 Simulation results of passenger car with front-wheel drive pattern

Pavement adhesion coefficient	Recovery rate	Braking distance [m]
0.3	2.68%	38.11
0.4	3.93%	28.60
0.5	5.15%	23.21
0.6	6.27%	19.90
0.7	7.23%	17.79
0.75	7.33%	17.39
0.8	7.33%	17.07
0.85	7.33%	16.80
0.9	7.33%	16.57

Table 5 Simulation results of commercial car with rear-wheel drive pattern

Pavement adhesion coefficient	Recovery rate	Braking distance [m]
0.3	1.29%	41.74
0.4	1.75%	31.58
0.5	2.17%	25.94
0.6	2.54%	22.62
0.7	2.75%	20.97
0.75	2.79%	20.55
0.8	2.79%	20.21
0.85	2.79%	19.93
0.9	2.79%	19.71

The results in the Table 4 and Table 5 indicate that the recovery rate increases with increment of pavement adhesion coefficient when the pavement adhesion coefficient is lower than 0.7. When the pavement adhesion coefficient is higher than 0.7, the recovery rate stays the same and it is the maximum value. When the pavement adhesion coefficient is 0.7, the recovery rate is lower than the maximum but is close to it. This is because there are some vibrations in the parallel strategy when the braking severity equals the threshold value (0.7). However, the theoretical analyses neglect these vibrations. In addition, it can be concluded from the results that the braking distance decreases with the increment of pavement adhesion coefficient.

6. Conclusion

The object of study is parallel hybrid electric vehicles. The impacts of pavement adhesion coefficient on the recovery rate and braking distance were analyzed. The conclusions are that the recovery rate increases with increment of pavement adhesion coefficient until the pavement adhesion coefficient reaches the value of 0.7 and then the recovery rate remains the same and that the braking distance decreases with the increment of pavement adhesion coefficient.

Acknowledgements

This work is supported by the National High-Tech Research and Development Program of China (863 Program) (Grant No.2012AA111003) and Technology Development Program of Weihai City (Grant No.2013DXGJ11).

References

- [1] Liu, Jinlong, Jingming Zhang, and Zhiwei Gao. "The Energy Management and Coordination in PHEV." *Journal of applied science and engineering innovation*, Vol 1.4 (2014).
- [2] Liu, Jinlong, Jingming Zhang, and Mingzhi Xue. "A Novel Parallel Regenerative Braking Control Strategy." *Journal of applied science and engineering innovation*, Vol 1. 4 (2014).
- [3] Liu, Jin Long, Zhi Wei Gao, and Jing Ming Zhang. "Analyses of the Relations Between Driving Types and Regenerative Braking in Electric Vehicles." *Advanced Materials Research*. Vol.926. 2014.
- [4] Liu, Jin Long, Jing Ming Zhang, and Ming Zhi Xue. "Analyses of Relations between Pavement Adhesion Coefficient and Regenerative Braking in Hybrid Electric Vehicles," *Applied Mechanics and Materials* 536 (2014): 1065-1068.
- [5] Zhang, Jing Ming, Jin Long Liu, and Ming Zhi Xue. "Analyses of the Relation Between Degree of Mixing and Regenerative Braking in Hybrid Electric Vehicles," *Advanced Materials Research*, Vol. 926. 2014.
- [6] Liu, Jinlong, Xiaoyu Zhang, and Rui Huang. " Impacts of PHEV Driving Types on Electro-hydraulic Braking," *Journal of Computational Science & Engineering*, Vol. 12. 2014.